Micro-CT Analysis of Tissue Engineering Scaffold Architectures

Ferry Melchels[1], Bart Rijckaert[1], Dirk Grijpma[1,2] and Jan Feijen[1]
1) Institute for Biomedical Technology (BMTI) and Department of Polymer Chemistry and Biomaterials, Faculty of Science and Technology, University of Twente, P.O. Box 217, 7500 AE, Enschede, The Netherlands
2) Department of Biomedical Engineering, University Medical Center Groningen and University of Groningen, P.O. Box 196, 9700 AD Groningen, The Netherlands
e-mail: f.melchels@utwente.nl

ABSTRACT SUMMARY
A novel method was developed for a quantitative assessment of pore interconnectivity using micro-CT data. This method makes use of simulated spherical particles, percolating through the interconnected pore network. For each sphere diameter, the accessible pore volume is calculated. This algorithm was applied to compare pore interconnectivity of two different scaffold architectures; one created by salt-leaching and the other by stereolithography. The algorithm revealed a much higher pore interconnectivity for the latter one.

INTRODUCTION
In tissue engineering, porous scaffolds are employed as temporal support structures that provides cells with surface area to adhere, proliferate and deposit extra-cellular matrix. These scaffolds also have to bear considerable mechanical loading in most in vivo applications. The architecture of the scaffold has a large influence on its mechanical properties. Also, an interconnected pore network is a necessity for efficient cell seeding and effective transport of nutrients and metabolites during culturing and after implantation. Porosity and pore size are frequently assessed structural parameters. Pore interconnectivity however, is mostly ignored or at best qualitatively evaluated[1]. This study applies micro-computed tomography (micro-CT) as a technique to asses structural parameters of the pore network inside scaffolds. Also, a novel algorithm has been developed that uses micro-CT data to evaluate pore interconnectivity in a quantitative manner, in terms of the accessible pore volume. This accessible pore volume is determined as the volume of the scaffold that can be reached from the exterior by simulating the percolation of spherical particles through the interconnected pore network.

EXPERIMENTAL METHODS
Poly(D,L-lactide) oligomers (1 kg/mol) were synthesized by ring opening polymerisation (130 °C, 40 h) of D,L-lactide starting from hexanediol as an initiator, and using stannous octoate as a catalyst. These oligomers were end-functionalised by reacting the terminal hydroxyl groups with methacrylic anhydride (120 °C, 8 h) and purified by vacuum distillation. Photo-polymerisable resins were obtained upon addition of photo-initiator and 20 wt% N-methyl pyrolidone (NMP) as a non-reactive diluent.
Porous scaffolds of similar porosity and pore size were obtained by either photo-polymerising the resin in the presence of 70 vol% NaCl particles (250-425 μm) and subsequent leaching in demi-water, or by stereolithography fabrication using a 70 % porous gyroid design and an EnvisionTec Perfactory Mini Multilens stereolithography apparatus. Both types of scaffolds were extracted in isopropanol/acetone mixtures and dried at 90 °C prior to characterisation.
Structural analysis of the porous scaffolds was performed using micro-computed tomography (μCT) scanning on a GE eXplore Locus SP scanner at 6.7 μm resolution. The scan was carried out at 80 kV voltage, 80 μA current and 3000 ms exposure time. GE Healthcare MicroView 2.2 was used to assess porosities and pore size distributions, and to generate a spacing map allocating a pore size to all pore volume elements (voxels) in the scanned data.
MathWorks Matlab R2007b was used to design two algorithms that were applied to the scanned data of the two porous scaffolds. The first generates a spacing map thresholded to a minimum pore size. The second uses this thresholded spacing map to determine the pore

volume that is interconnected to the exterior of the scaffold, by channels with a minimum diameter that corresponds to the applied pore size threshold.

RESULTS AND DISCUSSION

The methacrylate end-functionalised poly(D,L-lactide) macromers were synthesized with 96 % end-group conversion, as determined by proton nuclear magnetic resonance spectroscopy. Using the two different techniques both based on photo-polymerisation, porous scaffolds were obtained from these macromers. The scaffolds were scanned using micro-CT and the resulting data was used to calculate the structural parameters porosity, pore size and pore interconnectivity. Figure 1 shows visualisations of both scaffolds, based on the scanning data.

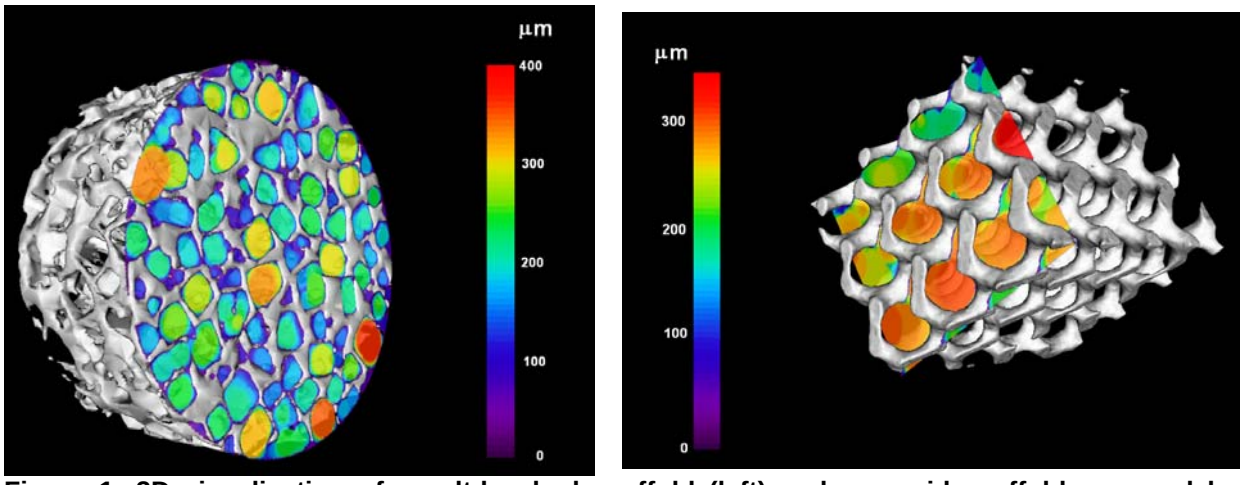

Figure 1: 3D visualisation of a salt-leached scaffold (left) and a gyroid scaffold prepared by stereolithography (right), both showing the pore size distribution in a particular cross-section

In the images, the pore size distribution in a particular cross-section is visualised. Figure 2 presents this pore size distribution as a histogram. When comparing both scaffold architectures, it is evident that the gyroid architecture has a much narrower pore size distribution. This follows from the regularity of the design that was employed. Also it can be seen that the average pore size for the gyroid scaffold is higher than that of the salt-leached scaffold (256 and 200 µm, respectively). The porosity is 79 % for the gyroid scaffold that was prepared using stereolithography, and 74 % for the salt-leached scaffold.

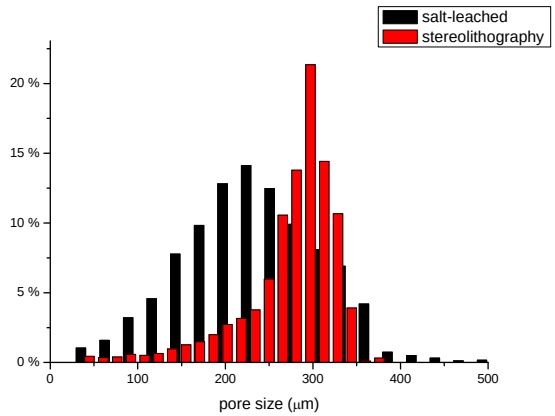

Figure 2: pore size distributions of both scaffold architectures

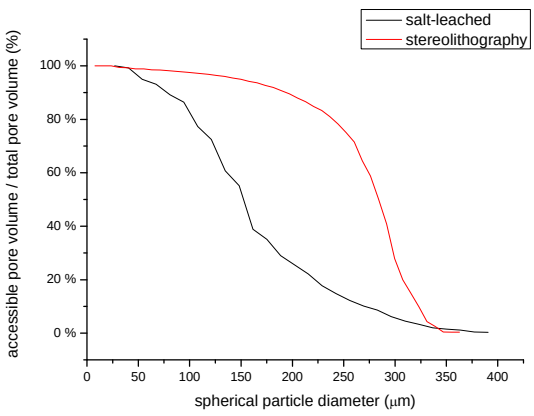

Figure 3: accessible pore volume fractions of both scaffold architectures

Figure 3 presents the results that were obtained using the new algorithm to quantify interconnectivity. It is evident that the regular gyroid architecture that was fabricated by stereolithography, has a better pore interconnectivity than the salt-leached structure. For example, when looking at a simulated spherical particle that has a diameter which corresponds to the average pore size, the accessible pore volume fraction is 25 % for the salt-leached structure and 75 % for the gyroid structure, respectively. This means that many pores in the salt-leached architecture are much larger than the channels that connect them to the exterior of the scaffold. This can be explained by the fact that interconnections between pores only occur at interfaces between two salt particles. In the gyroid, the pores are arranged in channels which have the same diameter throughout the scaffold. This results in a higher permeability of the gyroid scaffold, which is favourable for transport of nutrients and metabolites.

A limitation of the algorithm is that it assumes pores having a spherical geometry. As a result, pore voxels that do not lie in the largest sphere that fits in a non-spherical pore, are assigned a too small pore size[2]. This can be seen in the left-side tailing of the gyroid pore size distribution (Figure 3). However, in an interconnected pore network the boundaries of an individual pore can only be defined by assuming a particular pore geometry. The assumption of spherical pores enables a quantitative comparison of pore interconnectivity in tissue engineering scaffolds. In this comparing study of two dissimilar architectures, the intuitively accepted higher permeability for the regular gyroid structure has clearly come out, in a quantitative manner.

CONCLUSION

A novel algorithm was developed to asses pore interconnectivity of porous architectures based on micro-CT data. Application of the algorithm on two dissimilar scaffold structures revealed a much higher pore interconnectivity for the computer-designed gyroid structure that was built using stereolithography.

REFERENCES

1. Hutmacher, D.W., J.T. Schantz, C.X.F. Lam, K.C. Tan, and T.C. Lim, *State of the art and future directions of scaffold-based bone engineering from a biomaterials perspective.* Journal of Tissue Engineering and Regenerative Medicine, 2007. **1**(4): p. 245-260.
2. Hildebrand, T. and P. Ruegsegger, *A new method for the model-independent assessment of thickness in three-dimensional images.* Journal of Microscopy-Oxford, 1997. **185**: p. 67-75.

ACKNOWLEDGEMENTS

We would like to acknowledge the EU for funding (STEPS project, FP6-500465).